JOURNAL OF THE BALKAN GEOPHYSICAL SOCIETY, Vol. 13, No. 1, February 2010, p. 1-8, 6 figs, 1 table.

Integrated geophysical methods for imaging saline karst aquifers. A case study of Stylos, Chania, Greece

Hamdan Hamdan*, George Kritikakis, Nikos Andronikidis, Nikos Economou, Emmanouil Manoutsoglou and Antonis Vafidis

Technical University of Crete, Department of Mineral Recourses Engineering, Chania, 73100, Greece

(*hamdan@mred.tuc.gr)

(Received 03 October 2009; accepted 12 January 2010)

Abstract: *Geophysical methods are useful for mapping the boundary between fresh and saline water in coastal areas. However, the existence of karstic formations increases the uncertainty on geophysical sections and complicates the interpretation of geophysical data. In this paper, a systematic geophysical methodology for imaging saline water intrusion, in complex geological structure is being presented. We applied three methods for the inversion of resistivity data, as well as multi array data joint inversion and time lapse tomography. For the interpretation of the geophysical data we combined seismic velocity and resistivity sections. This integrated geophysical survey revealed saline water zones in the investigated area and verified that a major normal NE-SW fault zone is mainly responsible for the groundwater salinization in the Stylos area.*

Key words: *Electrical and seismic tomography, Saline karst aquifers, resistivity inversion, Stylos-Chania.*

INTRODUCTION

Geophysical methods have been used by many researchers to monitor salt water intrusion in coastal areas (Singh et al., 2004, Abdul Nassir et al., 2000, Lashkaripour, 2003, Gnanasundar and Elango, 1999, Imhof et al., 2001, Haxhiu and Uci, 1994, Prakash et al., 1980). The presence of dissolved chlorine ions in aquifers reduces dramatically their resistivity and thus electrical resistivity methods are very effective in locating salinization zones.

Although the seismic methods are unable to delineate directly the salinization, they can provide valuable information about the geological causes that favor the contamination of fresh water (Balia et al., 2003, Mela, 1997, Jarvis and Knight, 2002, Haeni, 1986).

The saline water in karstic formations contaminates the aquifers through a complex system of karstic or fractured carbonate rocks. The strong lateral inhomogeneity of such complex structures complicates the imaging and interpretation of geophysical data.

In this paper, we present the preliminary results of an integrated geophysical survey, for imaging saline karstic aquifers of Stylos (Chania, Crete, Greece) area. This survey combines VLF, electrical sounding, electrical tomography, seismic refraction and Multichannel Analysis of Surface Waves (MASW) methods in order to map the complex geology of the area.

SURVEY REGION

The springs of Stylos village, Crete, Greece (Fig. 1) play an important role in Chania irrigation water supply. In a water well near a polje located approximately 1300 m N-NW of Stylos village, saline (brackish) water was drilled in 1981-2. The absence of gypsum, anhydrite, or mineral salt in the area and the presence of faulted carbonate formations, indicates that the groundwater salinizaton is caused by seawater intrusion. The seashore is located north of the polje, at a distance of 2900 m (Fig. 1) (Hamdan et al., 2007).

A detailed hydrogeological survey was carried out in the region, combining information from boreholes, hydrogeological data (Zervogiannis and Xatziagorakis, 1969) and recent geological mapping (scale 1:5,000, Michalakis et al., 2006).

The western part of the area, covered by carbonates, consists of two major tectonic units: the lowermost Plattenkalk group and the brecciated carbonates of theTrypali unit. Poljes are observed on this later unit (Fig. 1). A major normal NE-SW fault is observed near the Aptera horst. Neogene marls and marly limestones are in contact with the Trypali carbonates along this fault and cover the eastern part of the investigated area (Fig. 1).

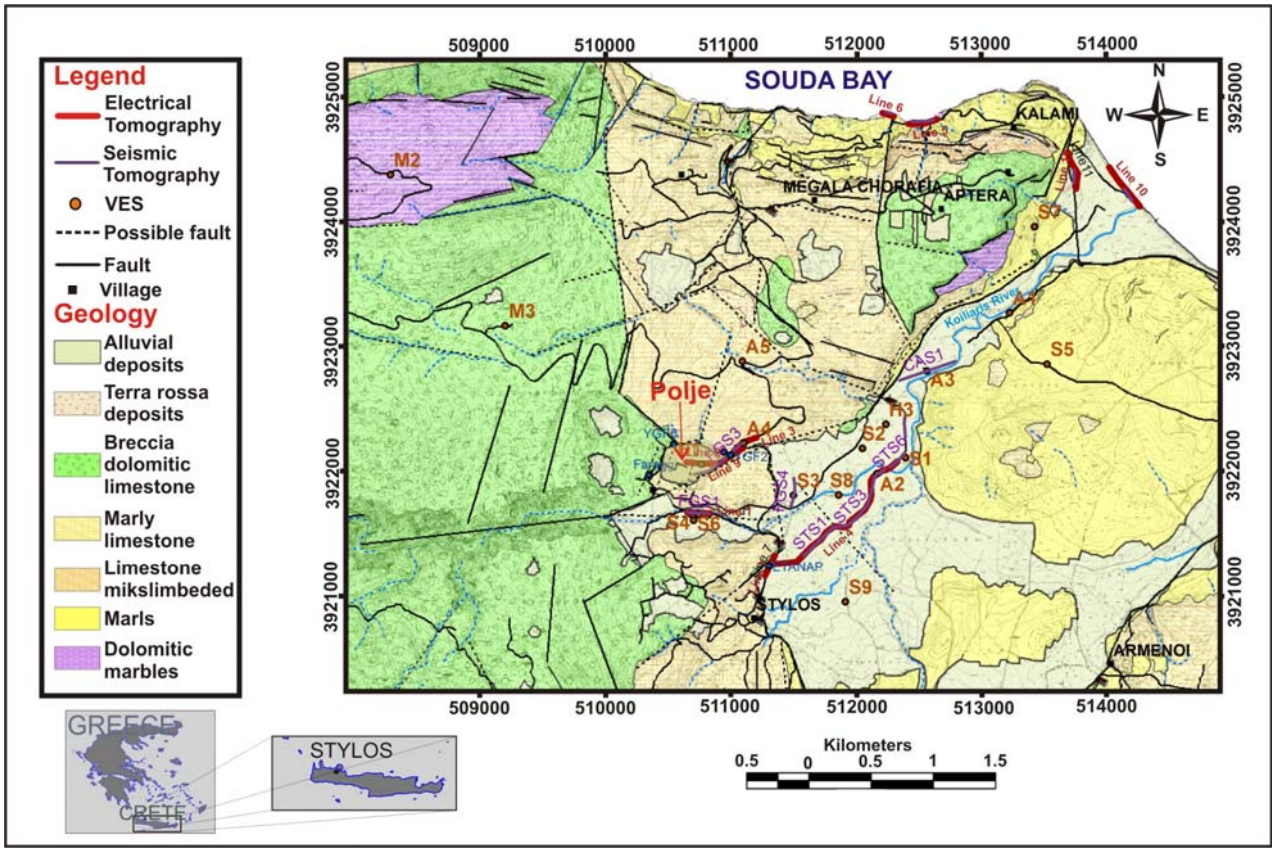

FIG. 1. Geological map of the investigated area. The location of the seismic and tomography lines and VES centers are also shown.

METHODOLOGY

For the design of the geophysical survey, several factors were taken into account, such as the area under investigation and the existing geological and hydrogeological information. The rough terrain and the requirements of increased investigation depths mainly in the western region also played an important role in designing this survey.

The geophysical survey was conducted in two phases. An initial reconnaissance survey delineated the regions of geological and hydrogeological interest. Based on the reconnaissance survey results, we conducted a high resolution survey, in order to image karstic features in the investigated area.

PHASE I: VES AND VLF SURVEYS

During this phase, we in situ estimated the resistivity values of the geological formations and we mapped the non visible faults in the region of interest. This phase provided all the necessary information for the planning of a detailed high resolution geophysical survey.

VLF scanned more than 10 km with station interval 5 m. Figure 2 displays a typical VLF profile and a map of the visible and non visible faults (blue dashed and continuous lines respectively) deduced from the VLF anomalies.

Twenty vertical electrical soundings (VES) covered the study area, using the Schlumberger array (Fig.1). The maximum current electrode spacing ranged from 140–1500 m. Table 1 presents the in situ measured resistivity values of the surveyed geological formations. The presence of karst in marly and Trypali limestones, saturated by fresh or saline water, explains the wide range of measured resistivities.

VES provided information about the thickness of the shallow geological formations and delineated low resistivity geoelectric layers attributed to water salinization. Figure 3 displays geoelectrical model of VES S5 which is located to the northeast of the studied area at elevation of 37 m. A very low resistivity zone, approximately at zero elevation, is attributed to the presence of saline water in marly limestones.

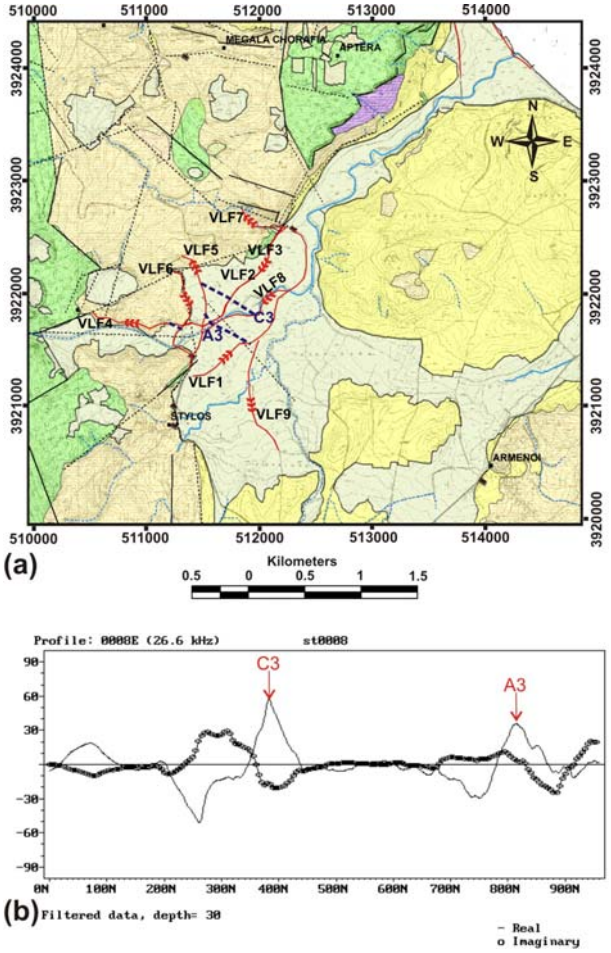

Fig. 2. VLF lines on the map of the investigated area (a) where dashed blue lines represent the revealed non visible faults deduced from the VLF anomalies (b).

Table 1. In situ resistivity values of the surveyed geological formations.

Geological formation	Resistivity range (ohm.m)
Plattenkalk	> 2000
Trypali limestones	500 – 3000
Marly limestones	100 – 700
Marls	40 - 80
clay	20 - 60

PHASE II: SEISMIC AND ELECTRICAL TOMOGRAPHY SURVEY

Seismic and electrical tomography methods provided images of the subsurface beneath selected areas of hydrogeological interest, according to the detailed geological map and the results of the reconnaissance (phase I) geophysical survey. The seismic methods mapped in detail the shallow geological formations, while the electrical tomography imaged the deeper structures detecting saline and karstic zones.

The seismic survey employed the methods of seismic tomography and MASW. The seismic survey aimed to delineate the subsurface geological formations and locate possible tectonic features (i.e. faults) which may favor the sea water intrusion. From the first arrivals of direct and head waves we obtained P-wave velocity sections, while by inverting the Rayleigh wave dispersion curves we calculated the shear wave velocity profiles. Twelve (12) seismic lines, with total length of 2715m, were surveyed using the 12-channel seismograph Geode (Geometrics), common source array and 4.5 Hz vertical component geophones. A 6kg sledge hammer and a seisgun produced seismic records. From these records we both picked first arrivals and extracted the dispersion curves used for processing with seismic tomography and MASW methods respectively.

The objectives of the electrical tomography survey are: a) to track the salinization front from the seashore towards the polje (Fig. 1), b) to map the polje complex geological structure and c) to image fractured, karstic and low resistivity zones, indicated by the detailed geological mapping.

Eleven (11) electrical tomography lines covered 3500 m using the Wenner-Schlumberger and dipole-dipole arrays (Fig. 1). The electrode spacing was set from 4 to 20 m. Sting R1/Swift AGI system collected apparent resistivity data which were subsequently inverted using RES2DINV software.

DATA PROCESSING AND INTERPRETATION

In order to reduce inversion uncertainty deduced from the complex geological structure of the region four approaches were employed: a) application of three inversion methods, b) multi array joint inversion of resistivity data, c) time lapse tomography and d) combined interpretation of seismic and resistivity sections.

Inversion of resistivity data

Three inversion techniques were applied on electrical tomography lines, namely: a) Smoothness constrained inversion (DeGroot-Hedlin and Constable, 1990), b) combined dumping and smoothing technique (Res2Dinv instruction Manual, 2006), and c) the blocky inversion (Claerbout and Muir, 1973, Wolke and Schwetlick, 1988).

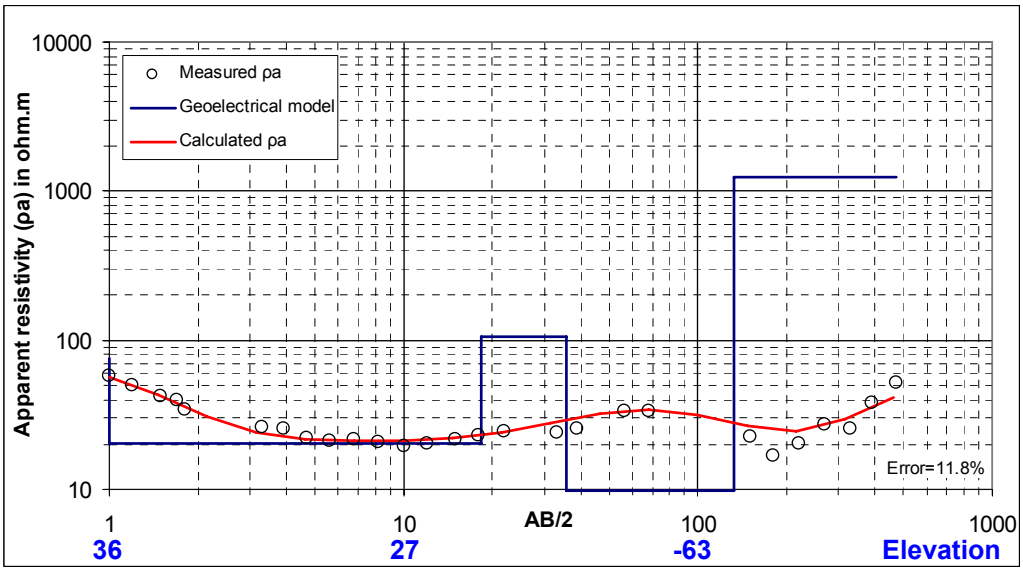

FIG. 3. VES S5 geoelectrical model. A very low resistivity zone is detected approximately at zero elevation.

The smoothness constrained inversion technique is the most commonly used, due to its fast convergence and quite satisfactory results. In this technique the resistivity values smoothly vary. This is not the case for karstic formations. The Combination of damping and smoothing techniques delineates large variation of resistivity values, especially if very low values are present (Loke, 2002), which is the case in the study region. However, the resultant resistivity sections (Fig. 4) are similar to those deduced from the smoothness constrained inversion.

Blocky inversion revealed a highly karstic formation, by enhancing sharp boundaries between homogeneous resistivity regions (Fig. 4) (Hamdan and Vafidis, 2009). Figure 4 (a and b) displays the resulted resistivity sections for electrical tomography Line 6, which is located near the seashore (Fig. 1), surveyed with the Wenner-Schlumberger (a) and Dipole-dipole (b) arrays.

The resistivity sections for the Wenner-Schlumberger data (Fig. 4a) are similar. These sections show a relatively higher resistivity layer (marls) overlaying a very low resistivity layer (strongly karstic Marly limestones saturated with saline water). The lateral inhomogeneity of the formations is better delineated in the Dipole-dipole sections (Fig. 4b), especially for the second geoelectric layer where the higher resistivity deeper geoelectric layer is attributed to marly limestones with reduced porosity.

Joint inversion of resistivity data

The advantages and disadvantages of different electrode arrays usage in electrical tomography have been well-studied (Ward, 1989, Loke 2002). The Wenner –Schlumberger array exhibits increased sensitivity to vertical resistivity variation (horizontal layers) and high signal to noise ratio, but suffers from poor resolution to lateral variations. On the contrary, the dipole-dipole array demonstrates increased resistivity resolution for mapping lateral changes, but is also sensitive to noise.

In a complex geology region, like the investigated area, both vertical and lateral resistivity variations are expected. A joint inversion of resistivity data collected using Wenner-Schlumberger and dipole-dipole arrays can delineate these resistivity variations (Stummer et al., 2004, de la Vega, 2003 Athanasiou et al., 2007).

Figure 4c shows the resistivity sections of the electrical tomography Line 6, deduced from the joint inversion of both arrays using the three inversion techniques mentioned above. The Dipole-dipole data mostly influence these sections which show better the boundaries between geolectrical layers. The blocky inversion employs more datum points than the other inversion techniques.

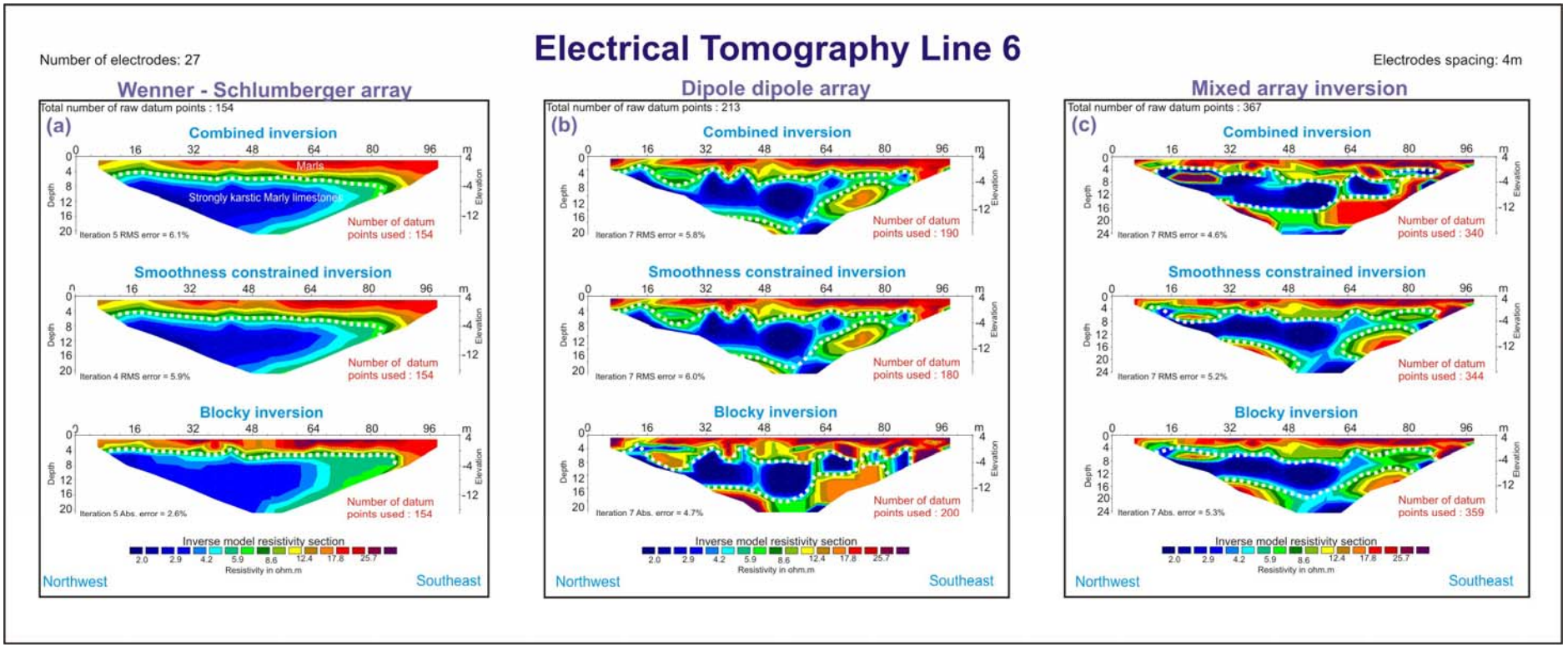

Fig. 4: Geoelectrical sections for line 6, deduced from different inversion methods for the Wenner-Shlumberger array data (a), the Dipole-dipole array data (b) and the mixed arrays data (c). White dotted lines indicate boundaries between resistivity layers.

Time lapse electrical tomography

A time-lapse geoelectrical experiment was realized in July 2005 and March 2006 along a 200m survey line 1 south of the polje (Fig. 1). The Wenner-Schlumberger array was utilized with 7 m electrode separation. Preliminary results indicate that the depth of the water layer do not encounter significant change throughout the year along the electrical tomography line (Fig. 5a).

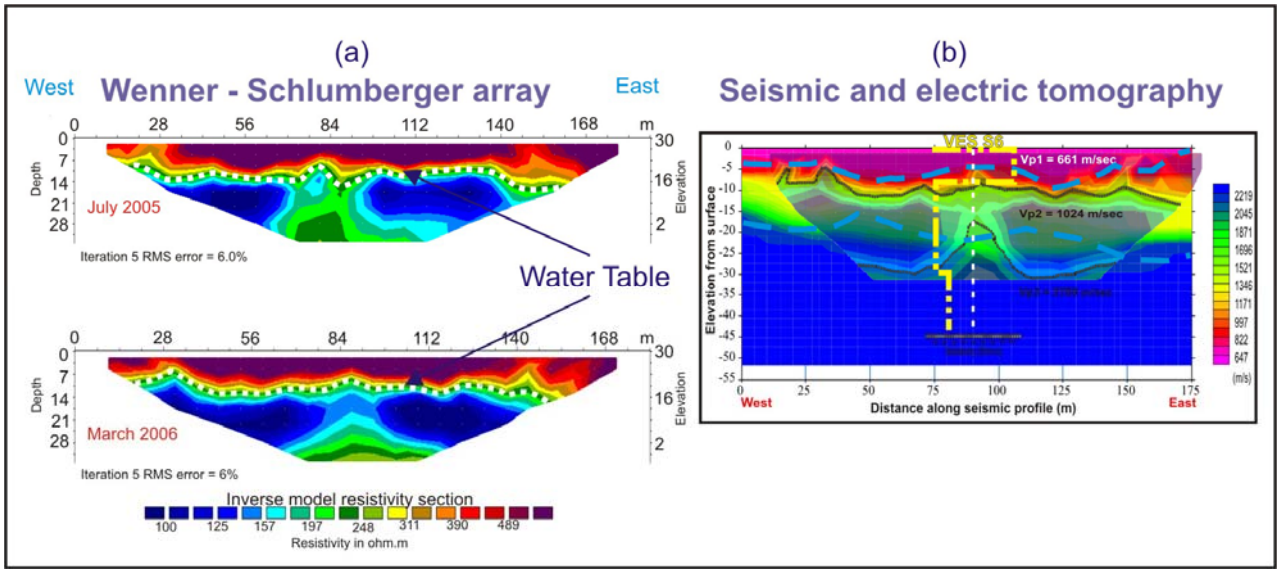

FIG. 5: Geoelectrical sections for Line 1 from two different seasons (a) and the results of superimposing geoelectrical section over the seismic section of line FGS1 (b).

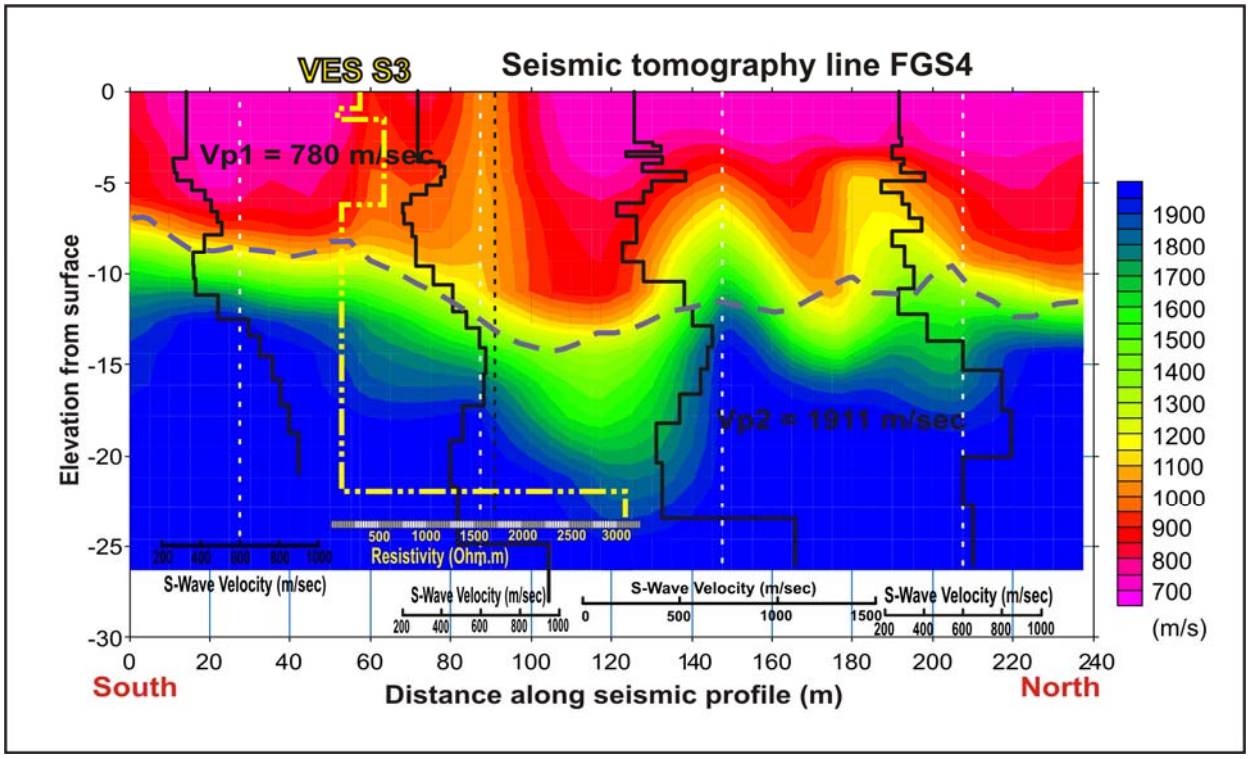

FIG. 6: Multichannel Analysis of Surface Waves (MASW) and VES 3 results superimposed on velocity depth section from seismic tomography FGS4.

Combined interpretation of seismic and resistivity sections

The combined interpretation of the geophysical sections involves superimposition of the seismic and resistivity sections, in order to compare the depths of the layers detected by the two methods.

Figure 5b shows the VES S6 geoelectrical model and the electrical tomography section Line 1 superimposed on the seismic section FGS1, which is located south of the polje (Fig. 1). Both electrical tomography and VES detect three geoelectrical layers. These layers are attributed to the marly limestones where the shallow layer is unsaturated while the deeper layers are saturated with fresh water. The increased resistivity of the third layer is due to the reduced porosity.

Although the seismic section detects three seismic layers also, their thickness is not in agreement with the thickness of the corresponding geoelectric layers. This can be explained by the fact that the seismic velocity is less influenced by the degree of saturation compared to the resistivity.

Furthermore figure 6 displays the geoelectrical model from VES S3 and the combined Vs profiles deduced from MASW method, superimposed on Vp seismic section FGS4 resulted from seismic tomography survey east of the polje. The geoelectrical model indicates the water table, while the seismic velocity section revealed two layers attributed to alluvial deposits and marly limestones.

CONCLUSIONS

Geoelectrical sections gave valuable information about the depth of water table and the presence of saline water, while seismic sections revealed zones of karstic carbonate formations in the investigated area of Stylos.

The results from the combined and smoothness constrained methods are similar in most electrical tomography lines in Stylos. Meanwhile, the blocky inversion sections are better, due to its ability to image sharp boundaries between resistivity zones, using the higher allowable number of datum points. The joint inversion of Wenner-Schlumberger and dipole-dipole data improves the electrical tomography sections in this complex geology region.

The combination of electric resistivity and seismic methods results in a powerful tool for imaging the saline water zone in karstic formations. This systematic geophysical methodology applied in this region, helped to overcome the difficulties in the interpretation of geophysical data from a complex geological structure. As a result of this investigation, a major normal NE-SW fault zone is mainly responsible for the groundwater salinization in the Stylos area.

ACKNOWLEDGMENTS

The authors would like to thank the PYTHAGORAS II project for the financial support of the geophysical and geological surveys and the Mineral Resources Engineering students of the 6th semester of the academic year 2005-2006, for helping in the geophysical field work.

REFERENCES

Abdul Nassir, S.S., Loke, M.H., and Nawawi, M.N., 2000, Salt-water intrusion mapping by geoelectrical imaging surveys: Geophysical Prospecting, 48, 647-661.

Athanasiou, E., Tsourlos, P., Papazachos, C., Tsokas, G., 2007, Combined weighted inversion of electrical resistivity data arising from different array types: Journal of applied geophysics, 62 (2), 124-140.

Balia, R., Gavaudo, E., Ardau, F., and Ghiglieri, G., 2003, Geophysical approach to the environmental study of a coastal plaijn: Geophysics, 68 (5), 1446-1459.

Claebout, J., and Muir, F., 1973, Robust modeling with erratic data: Geophysics, 38 (5), 826-844.

DeGroot-Hedlin, C., and Constable, S., 1990, Occam's inversion to generate smooth, two-dimensional models from magnetotelluric: Geophysics, 55 (12), 1613–1624.

De laVega, M., Osella, A., Lascano, E., 2003, Joint inversion of Wenner and dipole-dipole data to study a gasoline-contaminated soil: Journal of applied geophysics, 54 (2), 97–109.

Gnanasundar, D., and Elango, L., 1999, Groundwater quality assessment of a coastal aquifer using geoelectrical techniques: Journal of Environmental Hydrology, 7(17), 3411-3419.

Haeni, F.P., 1986, Application of seismic refraction methods in groundwater modelling studies in New England: Geophysics, 51. (2), 236-249.

Hamdan, H., Kritikakis, G., Vafidis, A., and Manoutsoglou, E., 2007, The role of

geophysical methods in salt-water intrusion mapping for strongly karst formations, a case study at Stylos, Chania, Greece: Proceedings of the 13th European Meeting of Environmental and Engineering Geophysics, 3–5 September 2007, Istanbul, Turkey.

Hamdan, H., and Vafidis, A., 2009, Inversion techniques to improve the resistivity images over karstic structures: Proceedings of the 15th European Meeting of Environmental and Engineering Geophysics, 3–5 September 2009 Dublin, Ireland.

Haxhiu, P., Uci, A., 1994, The determination of unpolluted underground water bounds in the Lushnja (Albania) seaside region: Publication of the academy of Finland, 4, 119-124.

Imhof, A.L., Guell, A.E., and Villagra, S.M., 2001, Resistivity sounding method applied to saline horizons' determination in Colonia Lloveras-San Juan Province-Argentina: Brazilian Journal of Geophysics, 19 (3), 263-278.

Jarvis, K.D., and Knight, R.J., 2002, Aquifer heterogeneity from SH-wave seismic impedance inversion: Geophysics, 67 (5), 1548-1557.

Lashkaripour, G.R., 2003, An investigation of groundwater condition by geoelectrical resistivity method: A case study in Korin aquifer, southeast Iran: Journal of Spatial Hydrology, 3(1), 1-5.

Loke, M.H., 2002, 2-D and 3-D electrical imaging surveys: tutorial.

Mela, K., 1997, Viability of using seismic data to predict hydrogeological parameters: Presented at SAGEEP, Reno/Sparks, Nevada.

Michalakis, I., Economou, N., Hamdan, H., Vafidis, A., Manoutsoglou, E., Panagopoulos, G., Roubedakis, S., Vozinakis, C., Lampathakis, S., and Dassyra, E., 2006, Geological and geophysical study of saltwater contamination at Stylos, Crete: Proceedings of the 2nd International Conference Advances in Mineral Resources Management and Environmental Geotechnology (AMIREG), 25 – 27 September, Chania, Greece.

Prakash, D., Kumar, K.V., and Tata, S.N., 1980, Geophysical studies for ground water exploration in Deccan Traps: Annual Convention and seminar on Exploration Geophysics, 25-26.

Res2Dinv instruction manual, ver.3.55, 2006, Geotomo software.

Singh, U.K., Das, R.K., and Hodlur, G.K., 2004, Significance of Dar-Zarrouk parameters in the exploration of quality affected coastal aquifer systems: Environmental Geology, 45 (5), 697-702.

Stummer, P., Maurer, H., and Green, A. 2004 Experimental design. Electrical resistivity data sets that provide optimum subsurface information: Geophysics, 69 (1), 120–139.

Ward, S., 1989, Resistivity and induced polarization methods: in Investigations in Geophysics No 5, Geotechnical and Environmental Geophysics, Vol. I, ed. S. Ward, SEG, Tulsa, 47-189.

Wolke, R., and Schwetlick, H., 1988, Iteratively reweighted least squares: Algorithms, Convergence analysis, and Numerical comparison: Siam J. Sci and Stat. Comput., 9 (5), 907-921.

Zervogiannis, G., and Xatziagoraki, D., 1969, Hydrological research in the region of Stilos- Armenwn-Kalivwn in the county of Chania: Ministry of Agriculture, Athens.